ACS APPLIED MATERIALS & INTERFACES
Research Article
www.acsami.org

Wafer-Scale Pattern Transfer of Metal Nanostructures on Polydimethylsiloxane (PDMS) Substrates via Holographic Nanopatterns

Ke Du, Ishan Wathuthanthri, Yuyang Liu, Wei Xu, and Chang-Hwan Choi*

Department of Mechanical Engineering, Stevens Institute of Technology, Hoboken, New Jersey 07030, United States

Supporting Information

ABSTRACT: In this paper, we report on a cost-effective and simple, nondestructive pattern transfer method that allows the fabrication of metallic nanostructures on a polydimethylsiloxane (PDMS) substrate on a wafer scale. The key idea is to use holographic nanopatterns of a photoresist (PR) layer as template structures, where a metal film is directly deposited in order to replicate the nanopatterns of the PR template layer. Then, the PDMS elastomer is molded onto the metal film and the metal/PDMS composite layer is directly peeled off from the PR surface. Many metallic materials including Ti, Al, and Ag were successfully nanopatterned on PDMS substrates by the pattern transfer process with no use of any adhesion promoter layer or coating. In case of Au that has poor adhesion to PDMS material, a salinization of the metal surface with 3-(aminopropyl)-triethoxysilane (APTES) monolayer promoted the adhesion and led to successful pattern transfer. A series of adhesion tests confirmed the good adhesion of the transferred metal films onto the molded PDMS substrates, including scotch-tape and wet immersion tests. The inexpensive and robust pattern transfer approach of metallic nanostructures onto transparent and flexible PDMS substrates will open the new door for many scientific and engineering applications such as micro-/nanofluidics, optofluidics, nanophotonics, and nanoelectronics.

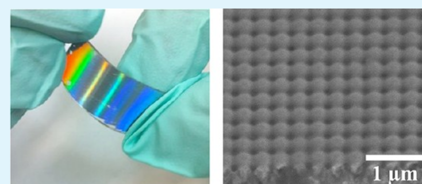

KEYWORDS: *pattern transfer, nanostructures, metal, PDMS, holographic nanopatterns, adhesion*

1. INTRODUCTION

Subwavelength periodic metallic nanostructures have many applications in micro-/nanosciences and technology, including micro-/nanofluidics,[1−3] nanoimprint lithography,[4,5] nanophotonics,[6] plasmonic devices,[7,8] and sensors.[9,10] A reliable and effective patterning method for metals is essential in the fabrication of such functional nanostructures and devices. Moreover, there is an increasing interest in developing micro-/nanosystems such as MEMS/NEMS and nanoelectronics devices on a soft and ductile substrate for flexible, stretchable, and wearable devices.[11−14] Among the flexible substrates, polydimethylsiloxane (PDMS) is widely used in such systems because of good transparency and ductility.[15] PDMS is also known as a biocompatible polymer, enabling the applications to microfluidics, lab-on-a-chip, and biomedical devices.[16] In order to create such metallic nanostructures and devices on flexible PDMS substrates, many fabrication techniques have been explored, including dry etching,[17,18] lift-off,[19] and printing/stamping.[20−24] Dry etching of metallic materials generally involves the use of toxic (chlorine or fluorine based) gases in a high vacuum environment, requiring expensive instrumentation and cleanroom working conditions. Furthermore, hindered by the native metallic oxide layer readily formed on the metal surface, the dry etching of metallic substrate is a difficult process.[17,18] Lift-off is a well-established and popular method to pattern metallic micro-/nanostructures using a photoresist mask layer on typical substrate materials such as silicon. However, on PDMS substrates, the delamination of a photoresist mask layer is a serious issue due to the poor adhesion between photoresist material and PDMS. The mismatch of the thermal expansion coefficients between photoresist and PDMS also typically results in mechanical cracks on the film when curing the photoresist.[19] Thus, intermediate layers should normally be used between the PDMS substrate and photoresist layer to promote the adhesion and relax the thermal problem. However, most intermediate layer materials, such as poly(acrylic acid) (PAA),[19] are not readily removable in the lift-off process, which makes the fabrication process much more complicated. In printing/stamping processes, the preparation of a separate mold or master structure is required for the replication, which also increases the complexity of the whole fabrication process.[20−24] Considering all these technical and practical issues, the development of an easier and more reliable fabrication technique is still essential to successfully pattern the nanostructures of various metallic materials on PDMS substrates.

In this paper, we demonstrate a simple and inexpensive, robust and reliable pattern transfer technique capable of large-area (wafer-level) nanopatterning of various metallic nanostructures onto PDMS substrates. In our previous report,[25] we demonstrated a large-area pattern transfer method of metallic

Received: July 23, 2012
Accepted: September 28, 2012
Published: September 28, 2012

© 2012 American Chemical Society

nanostructures onto glass substrates by using a predefined nanostructured photoresist layer as a mold and then a sacrificial etching layer in the series of deposition and release processes for the replication and transfer of metallic nanostructures. Compared to the other pattern transfer methods that also typically require complicated nanofabrication or replication processes for the preparation of the mold structures themselves, such as using hard substrate material, Si or SiO_2,[26,27] or flexible soft material, poly(urethane acrylate),[28,29] as a mold template, the direct use of a photoresist film as a transfer layer has enabled the precision of pattern transfer to be increased and simplify the fabrication processes significantly. In this study, we advance such a pattern transfer technique to a PDMS substrate and develop a new pattern transfer process tailored for the PDMS substrate material. We also discuss the technical challenges associated with the proposed pattern transfer method for the PDMS substrate material, such as adhesion and sticking issues which are key physical parameters for the successful pattern transfer process.

2. FABRICATION SCHEME AND EXPERIMENTAL DETAILS

Figure 1 illustrates the proposed fabrication process. The key idea of the new fabrication process is to directly mold the PDMS elastomer onto the metallic film that is predeposited on a nanostructured photoresist layer and then mechanically peel off the composite layers

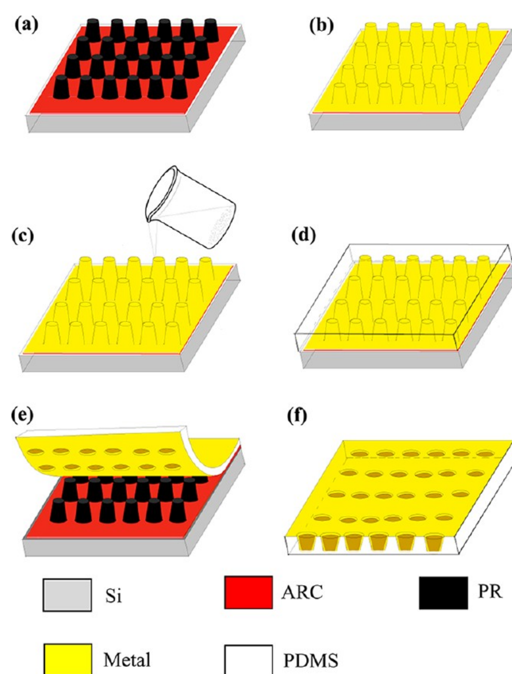

Figure 1. Schematic of a pattern transfer process of metal nanostructures onto a PDMS substrate. (a) Photoresist (PR) nanopatterns fabricated on a silicon (Si) substrate by using laser interference lithography. An antireflective coating (ARC) layer is used between the PR layer and the Si substrate to minimize the standing wave effects on the sidewall profile of the PR nanostructures. It also allows the development of high-aspect-ratio nanostructures of the PR. (b) Deposition (e.g., e-beam evaporation) of a metal film on the PR layer. (c) Molding of PDMS elastomer on the metal layer. (d) Curing of the PDMS layer to form a planar substrate. (e) Detachment (mechanical peeling) of the composite PDMS/metal layer from the PR surface. (f) The metal nanostructures transferred onto the PDMS substrate.

of metal/PDMS from the photoresist template surface. The details of the fabrication process are described in the following.

First, a large-area nanopatterned photoresist (PR) layer is prepared on a silicon (Si) substrate by using laser interference lithography (Figure 1a). Before the lithography, a polished Si wafer was cleaned with acetone and deionized (DI) water and then dried by the blow of nitrogen (N_2) gas. Then, antireflective coating (ARC) was spun on the bare Si wafer. The ARC layer is applied to reduce the vertical standing-wave effects caused by the reflection of light from the polished silicon surface at the exposure in lithography. Otherwise, the vertical standing wave induces sinusoidal roughness (scalloping) along the sidewall profile of the PR nanostructures and adversely affects the pattern transfer process, especially in the peeling step of the metal film from the PR layer (Figure 1e), resulting in sticking and mechanical fracturing. For the ARC, the XHRiC-16 (Brewer Science) was spin-coated for 30 s at 2000 rpm to have the film thickness of 200 nm. The ARC layer was then baked on a hot plate at 175 °C for 1 min. Then, a PR layer was spun on the ARC layer. For the nanograting and nanopillar mold structures, a positive-tone resist (PR-500, Futurrex, Inc.) was used. For the nanoporous mold structures, a negative-tone resist (NR7-250, Futurrex, Inc.) was used. The PR solution was spin-coated for 30 s at 6000 rpm to have the film thickness of ~450 nm. After the spin-coating, the Si substrate was soft-baked on a hot plate, at 110 °C for 6 min for positive PR and 150 °C for 1 min for negative PR, respectively. The PR layer was then exposed by laser interference lithography system. Interference lithography is a maskless holographic lithography technique that can pattern sub-100 nm periodic nanostructures in a large area (up to a meter scale) in an inexpensive and efficient way.[30−32] In this experiment, we use "two degrees-of-freedom" Lloyd-mirror system,[33,34] which is an improved system over the conventional Lloyd-mirror interferometer, in order to have a larger pattern coverage area. Interference of two laser beams produces one-dimensional (1D) nanograting patterns by a single exposure or two-dimensional (2D) nanogrid patterns by double exposures with an interim sample rotation by 90°. In case of using positive-tone PR, pillar-type structure is generally obtained in the double exposures, while pore-type structure would be with negative-tone PR. The periodicity of the nanopattern array is conveniently controlled by regulating the angle between the two interfering lights or the wavelength of the laser source. Two laser sources were used to produce different pattern coverage areas, including He−Cd (IK3501R-G, Kimmon Electric) and Ar-ion (Sabre 7, Coherent). The He−Cd laser (50 mW and 30 cm coherence length at 325 nm wavelength) was used to pattern a relatively small substrate area (less than 2-in. substrate), whereas the Ar-ion laser (1.7 W and 1 m coherence length at 351.1 nm wavelength) was used to pattern a larger area up to 4-in. substrate. To register grating and pillar patterns on the positive PR, a total of 80 mJ (single exposure) and 120 mJ (double exposures with 60 mJ for each) were exposed on the PR layer, respectively, regardless of the pattern periodicity. In the case of patterning pore patterns with the negative PR, 10 mJ (double exposures with 5 mJ for each) was used for the exposure. For the development of the exposed PR layer, a developer solution (RD6, Futurrex, Inc.) was used after being diluted with DI water at a ratio of 3:1 in volume. The positive PR layer was developed for 15 s, while the negative PR layer was for 10 s. They were then rinsed with deionized water for 60 s and blown dry with N_2 gas.

After the nanopatterning of a PR layer, a thin metal film is directly deposited on top of the PR/ARC layer (Figure 1b), e.g., by using e-beam evaporation (PVD-75, Kurt J. Lesker Company), which allows the deposition of various metallic films conformably and uniformly over the PR/ARC surface.[25] Before deposition, the base pressure of the chamber was set at $\sim 1 \times 10^{-7}$ Torr. The deposition rate for the metals (Ti, Al, Ag, and Au) was regulated to be 0.2 nm/s. During the deposition, the chamber pressure was maintained lower than 1×10^{-5} Torr.

Then, PDMS elastomer is directly molded and cured on the metal surface (Figure 1c). Sylgard 184 (Dow Corning Corporation) PDMS elastomer was used for the molding process. The PDMS base was first mixed with curing agent with a ratio of 10:1 in volume. The PDMS mixture was then poured on the metal surface and put in a vacuum

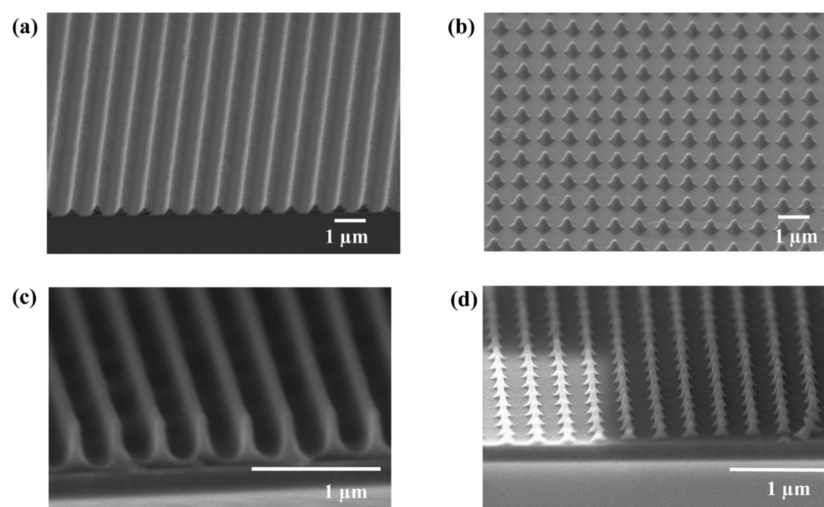

Figure 2. Scanning electron microscope (SEM) images of the PR mold patterns. (a, b) Grating and pillar patterns with a periodicity of 935 nm, respectively. (c, d) Grating and pillar pattern with a periodicity of 325 nm, respectively.

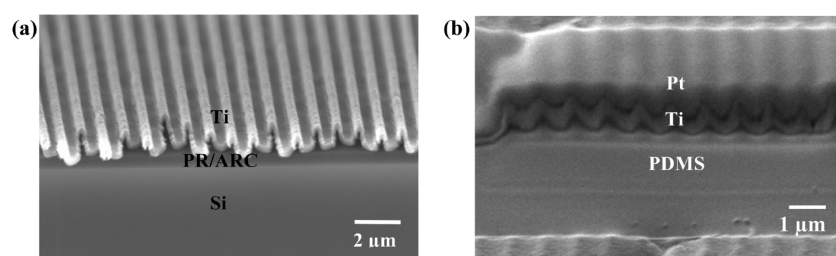

Figure 3. (a) SEM image of titanium (Ti) film (150 nm thick) deposited on the grating patterns (935 nm in periodicity) of the PR/ARC layer on a Si substrate. (b) SEM image of the Ti film transferred onto a PDMS substrate. Platinum (Pt) layer was deposited on the Ti layer for the focused ion beam (FIB) milling to show the cross-sectional image of the Ti film transferred on the PDMS substrate more clearly.

chamber with a base pressure at 10^{-6} Torr for ~1 h in order to purge the air bubbles that would be entrapped at the interface between the metal and PDMS (Figure 1d). The degassing time longer than 30 min normally produced uniform molding and adhesion of the PDMS elastomer to the metal surface. Following the degassing, the PDMS-covered sample was cured on a hot plate for 4 h at 60 °C.

Finally, the PDMS layer is mechanically peeled off from the Si substrate by hands for the transfer of metal film onto the PDMS surface (Figure 1e). The mechanical peeling provides a simple way of the release of the metal/PDMS composite layer from the PR/ARC surface and finishes the pattern transfer process (Figure 1f).

The new fabrication method has several advantages over the other pattern transfer techniques reported so far.[26−29] First, the lithographic PR patterns are directly used as a template mold, and the metallic material of interest is directly deposited onto the PR lithographic patterns. Therefore, no additional fabrication steps such as etching, deposition, or replication are necessary to prepare the mold structures of other materials. The use of laser interference lithography in the preparation of the PR holographic nanopatterns also allows the large-area (wafer-scale) pattern transfer. Second, the PDMS substrate is prepared by directly molding the liquid-phase PDMS elastomer onto the metal film, which does not require any special pressurizing or heating step to promote the adhesion. Third, the final release process does not require any sacrificial etching of the mold layer so that the PR template structure can be reused multiple times for the repetitive replication, which will enhance the fabrication throughput and lower the manufacturing cost furthermore.

3. RESULTS AND DISCUSSION

PR Mold Nanostructures. Figure 2 shows the PR nanostructures fabricated and tested as mold layers for the deposition and transfer of metal films. By using the "two degrees-of-freedom" Lloyd-mirror interferometer,[33,34] the uniform nanoperiodic array of PR patterns of the periodicity from 170 nm to 1 μm could be easily defined on a large area (up to a 4-in. wafer level), including nanograting, nanopillar, and nanopore patterns. Figure 2 shows the nanograting (Figure 2a,c) and nanopillar (Figure 2b,d) patterns of a period of 935 and 325 nm, respectively, made of positive-tone PR. The structural height, aspect ratio, and sidewall profile of the PR patterns are controllable by regulating the lithography conditions such as PR film thickness, exposure dosage, and development time. The structural height of the PR patterns shown in Figure 2 is all ~450 nm, making the aspect ratio varying from one (Figures 2a,b) to three (Figures 2c,d). The sidewall profile of the PR nanopatterns shown was modulated to be positively tapered, which allows the peeling of a metal film from the PR layer more reliable and nondestructive at the release step of the pattern transfer process.

Metal Deposition and PDMS Molding. Various metal materials (Ti, Al, Ag, and Au) were deposited by e-beam evaporation onto the PR mold nanostructures for the experiment of pattern transfer. Figure 3a shows the titanium (Ti) film (150 nm thick) deposited on the nanograting PR structures of 935 nm in periodicity. In the e-beam evaporation of metal films, the deposition rate was controlled to be less than 0.2 nm/s, which resulted in the conformal deposition of the metal film along the PR patterns. A higher deposition rate affected the uniformity and step coverage of the metal film so that the replica of metal film could not duplicate the genuine geometry of the PR mold structure accordingly.

dx.doi.org/10.1021/am301423s | ACS Appl. Mater. Interfaces 2012, 4, 5505−5514

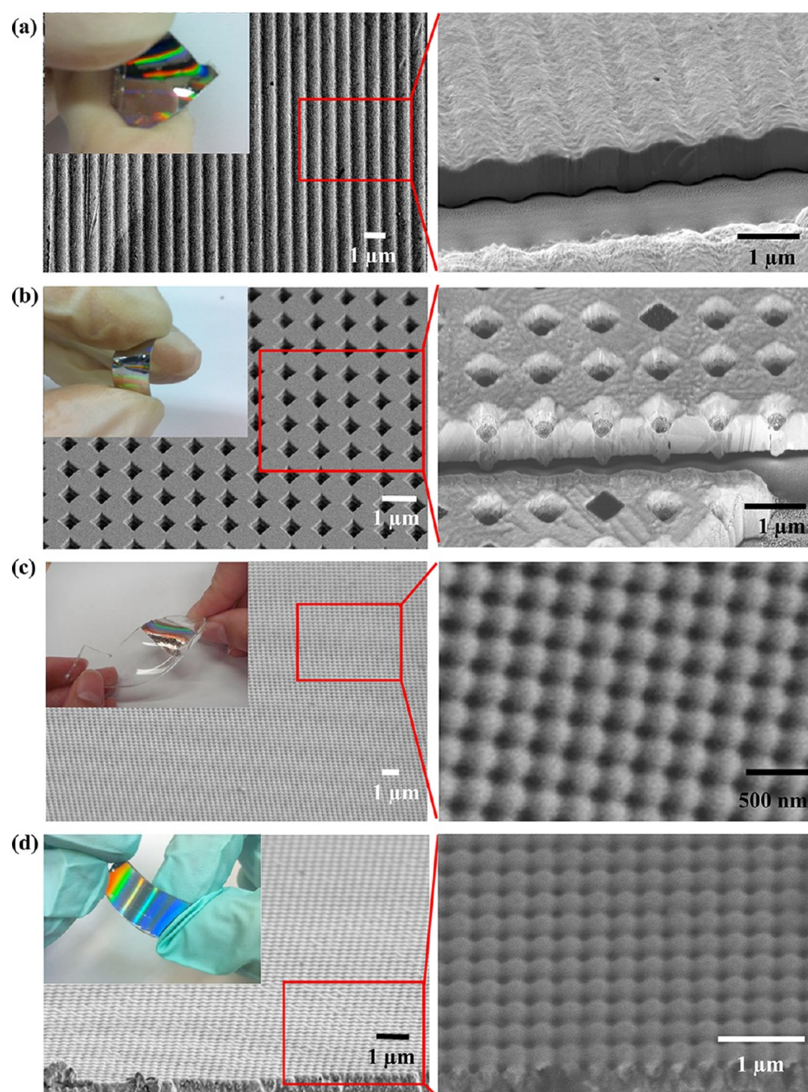

Figure 4. (a) SEM images of silver (Ag) grating structures transferred from the PR patterns shown in Figure 2a. (b) SEM images of Ag pore structures transferred from the PR patterns shown in Figure 2b. In (a, b), the images in a right column show the cross-sectional views of the metal layers after FIB milling. (c, d) SEM images of Ti and Al pore structures transferred from the PR patterns shown in Figure 2d, respectively. The inset of each image in a left column shows the nanostructured PDMS substrate with the mechanical bending applied by hands.

PDMS elastomer (Sylgard 184) was then poured in its viscous liquid form and solidified on the deposited metal surface. The effect of a volume ratio of a curing agent in the mixture of PDMS solution was examined on the adhesion to the metal surface as well as the fidelity of the pattern transfer. It was found that when the volumetric ratio was greater than 10:1, the adhesion between PDMS and metal was poor so that the quality (e.g., coverage and uniformity) of metal nanostructures transferred onto the PDMS substrate were severely affected by the concentration. In contrast, when the ratio was between 10:1 and 5:1, the PDMS showed good adhesion to the metal surface and the uniform pattern transfer of the nanostructured metal film (fidelity of ~100%) was achieved onto the PDMS, with no significant dependency on the concentration. Figure 3b shows the Ti nanostructures successfully transferred onto the PDMS substrate, after mechanically peeling off the PDMS layer from the Si substrate by hands, without using any etchant. To confirm the good contact between the PDMS substrate and the transferred metal layer, the interface between the metal and PDMS layers was examined by using focused ion beam (FIB) milling in the SEM (Auriga, Carl Zeiss NTS). A 10 μm × 5 μm area was milled by using Ga+ ions. The depth of milling was 500 nm. Before the FIB milling, 200-nm thick platinum (Pt) was deposited on the Ti surface in order to protect the Ti surface from damaging by high energy Ga+ ions and to have a clear image of the cross-sectional view of the interface between the Ti and PDMS. The result shows that the PDMS layer follows the corrugations of the nanostructured metal film accordingly and has good bonding with the conformal contact.

Metal Nanostructures Transferred on PDMS. Figure 4 shows the various metal nanostructures transferred onto PDMS substrates, including silver (Ag), titanium (Ti), and aluminum (Al). Figure 4a,b shows the Ag nanograting and nanopore structures fabricated by using the PR mold patterns (935 nm in periodicity) shown in Figure 2a,b, respectively. Figure 4c,d shows the Ti and the Al nanopore structures fabricated by using the nanopillar PR structures (325 nm in periodicity) shown in Figure 2d, respectively. In each image, the inset shows the optical micrograph of the mechanical manipulation of the nanostructured metal film on the PDMS substrate by hands.

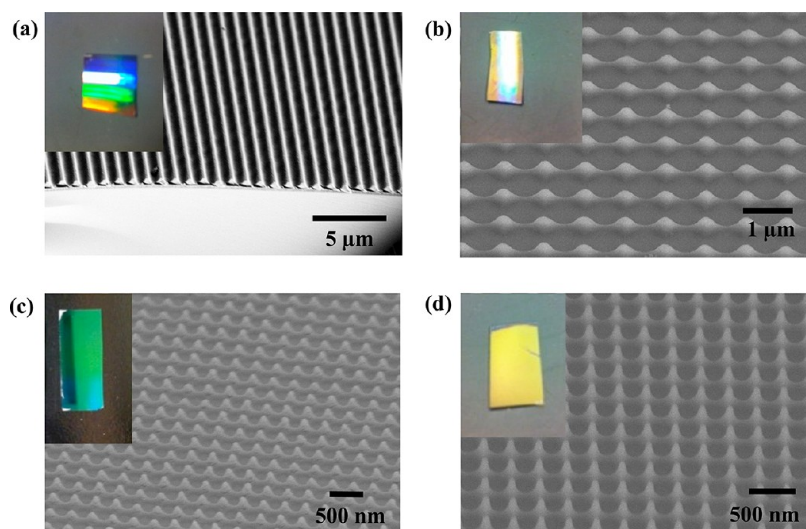

Figure 5. (a) SEM image of the PR mold patterns (935 nm in period) after the pattern transfer of Ag grating structures as shown in Figure 4a. (b) SEM image of the PR mold patterns (935 nm in period) after the pattern transfer of Ag pore structures as shown in Figure 4b. (c) SEM image of the PR mold patterns (325 nm in period) after the pattern transfer of Ti pore structures as shown Figure 4c. (d) SEM image of the PR mold patterns (325 nm in period) after the pattern transfer of Al pore structures as shown Figure 4d. The inset of each image shows the optical image of the PR surface of a whole sample.

Even with the mechanical deformation such as bending and twisting, the nanostructured metal films on the PDMS substrate do not show any noticeable delamination or crack, suggesting good adhesion between them. When such mechanical stresses were applied multiple times repetitively, significant cracks were often observed. However, no significant delamination was still observed even in such a case. The colors shown in the optical images represent the diffraction of light from the nanostructured metal surface. In Figure 2a,b, the high magnification SEM images show the cross sections of the metal films after FIB milling in the SEM. The results further demonstrate that the metal nanostructures replicate the PR mold nanopatterns with high fidelity (~100%). Moreover, no trace or residue of PR was observed on the metal surface after the transfer. It suggests that the metal nanostructures can be utilized immediately with no cleaning process. Such precise pattern transfer with good mechanical flexibility and robustness of the metal nanostructures would be of great benefit to the applications of flexible and wearable electronics.

PR Mold Nanostructures after Transfer Process. Figure 5 further shows the PR mold nanostructures retained on Si substrates after the transfer processes of the metal layers shown in Figure 4. The colors of the PR surfaces shown in each inset represent the diffraction of light due to the original nanopatterns of the PR surfaces. Compared to the initial geometries and dimensions of the PR nanostructures shown in Figure 2, no significant destruction or deformation of the PR mold nanostructures was detected even after the transfer process. It suggests that the PR nanostructures can be repetitively used for multiple replications as robust mold structures.

Transfer of Gold Nanostructures on PDMS. As demonstrated in Figure 4, most of metallic materials could be directly transferred from the PR mold layer to the PDMS substrate with no surface treatment step such as applying adhesion promoting layers or coatings between the metal and PDMS layers. However, in the case of gold (Au), it was difficult to release and transfer the deposited film from the PR layer to the PDMS surface directly, because of the poor adhesion between gold and PDMS material.[35] In order to promote the adhesion between gold and PDMS elastomer, intermediate adhesion layers such as Ti and Cr have been typically used in micro-/nanofabrication[36] and pattern transfer.[37,38] However, in our pattern transfer process for PDMS substrate, such interlayers (both Ti and Cr) did not help to improve the pattern transfer result of the Au film. It is attributed to the stronger adhesion between the Au and PR layers than that between the interlayer material and PDMS. Thus, instead of using physical thin films, we adopted the chemical treatment such as self-assembled monolayer coating for salinization. Salinization has been widely utilized to improve the adhesion of gold, such as using $-NH_2$ or $-SH$ functional groups.[39−42] In our experiments, we used 3-(aminopropyl)-triethoxysilane (APTES) which contains the $-NH_2$ functional group as a binder to improve the adhesion between the Au layer and PDMS matrix (Figure 6). First, APTES was prepared by diluting 1 mL APTES with 10 mL ethanol. The solution was agitated for 10 min and then spin-coated on a gold surface (2000 rpm, 30 s) (Figure 6a). Due to the high affinity between the gold surface and the $-NH_2$ group, a monolayer of APTES film (~1 nm thick) self-assembles on the Au surface with the $-OR$ group heading outside. Then, the surface was kept in ambient environment (55% RH) for 10 min for the hydrolysis of APTES on gold surface, where the $-OR$ group transforms to a $-OH$ group. The surface was then baked on a hot plate at 60 °C for 10 min (Figure 6b) to accelerate the hydrolysis and condensations of the APTES. Afterward, PDMS prepolymer was poured onto the functionalized Au surface and vacuumed for ~1 h to remove air bubbles (Figure 6c). The sample was then heated at 65 °C for 4 h to solidify the PDMS gel, where the $-OH$ group on the binding layer reacts with the $-OH$ groups of the PDMS, resulting in strong bonding between the gold layer with PDMS matrix. Finally, the Au nanostructures were transferred onto the PDMS substrate by mechanical peeling-off process (Figure 6d). Figure 6e shows the nanopillar PR structures used as a mold for the experiment. Figure 6f shows the Au nanostructures successfully transferred on the PDMS substrate by using the PR nanopattern as a mold. By applying the chemical functionalization of gold with the

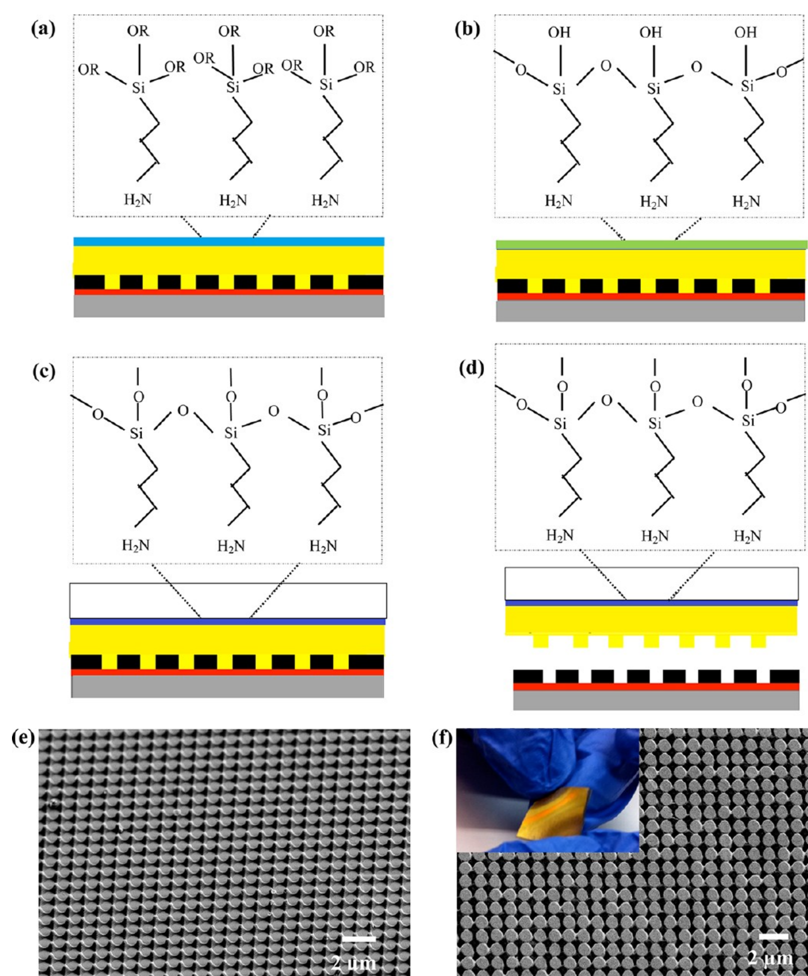

Figure 6. (a−d) Schematic of a pattern transfer process of gold (Au) nanostructures on a PDMS substrate: (a) Before PDMS molding, 3-(aminopropyl)-triethoxysilane (diluted with ethanol) is spin-coated on the gold surface. (b) The sample is exposed in ambient environment and baked for the transformation of the −OR function group to −OH. (c) PDMS is molded on the sample surface, where the −OH group transforms to −O− and results in strong bonding with PDMS. (d) The composite gold/PDMS layer is peeled off from the PR surface. (e, f) Fabrication results: (e) SEM image of the PR patterns used as mold. (f) SEM image of the Au patterns transferred onto a PDMS substrate. In (e), the inset shows the optical image of the nanostructured PDMS substrate with mechanical bending by hands.

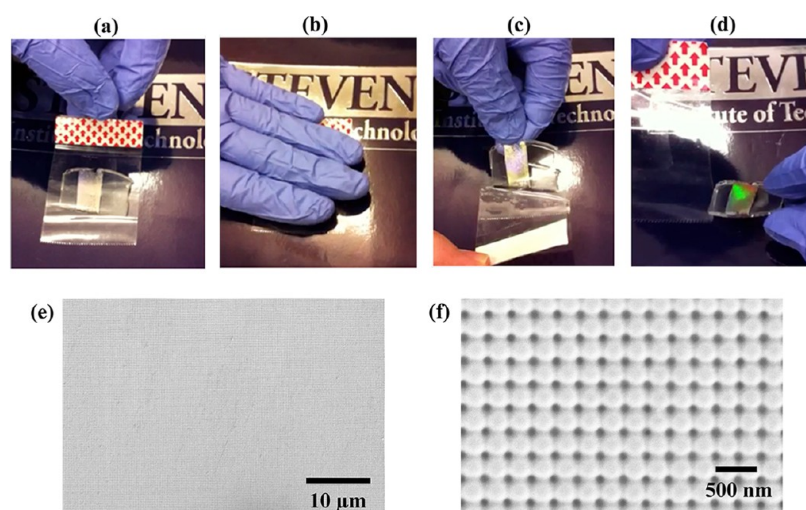

Figure 7. Scotch-tape adhesion test: (a) A scotch tape is applied on a PDMS substrate (2 in. × 2 in.) patterned with Ti nanostructures. (b) Mechanical pressure is applied on the tape by hands. (c) The tape is removed by hands. (d) No delamination of Ti layer is observed on the surface. (e, f) SEM images of the Ti surface after the scotch-tape peel-off test, showing neither microscale crack of the film nor nanoscale destruction of the structures.

dx.doi.org/10.1021/am301423s | *ACS Appl. Mater. Interfaces* 2012, 4, 5505−5514

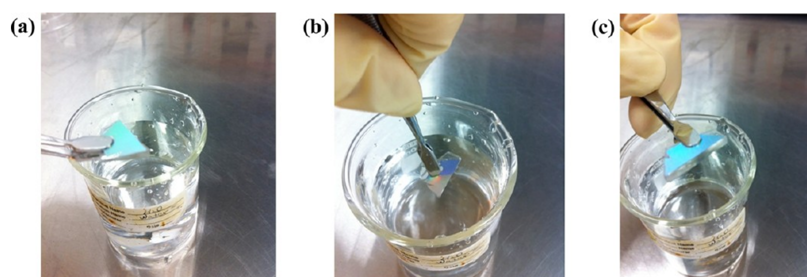

Figure 8. Immersion test in water. (a) The PDMS substrate patterned with Ti nanostructures is immersed in deionized water. (b) After 7 days, the sample is taken out. (c) No delamination of Ti layer is observed on the surface.

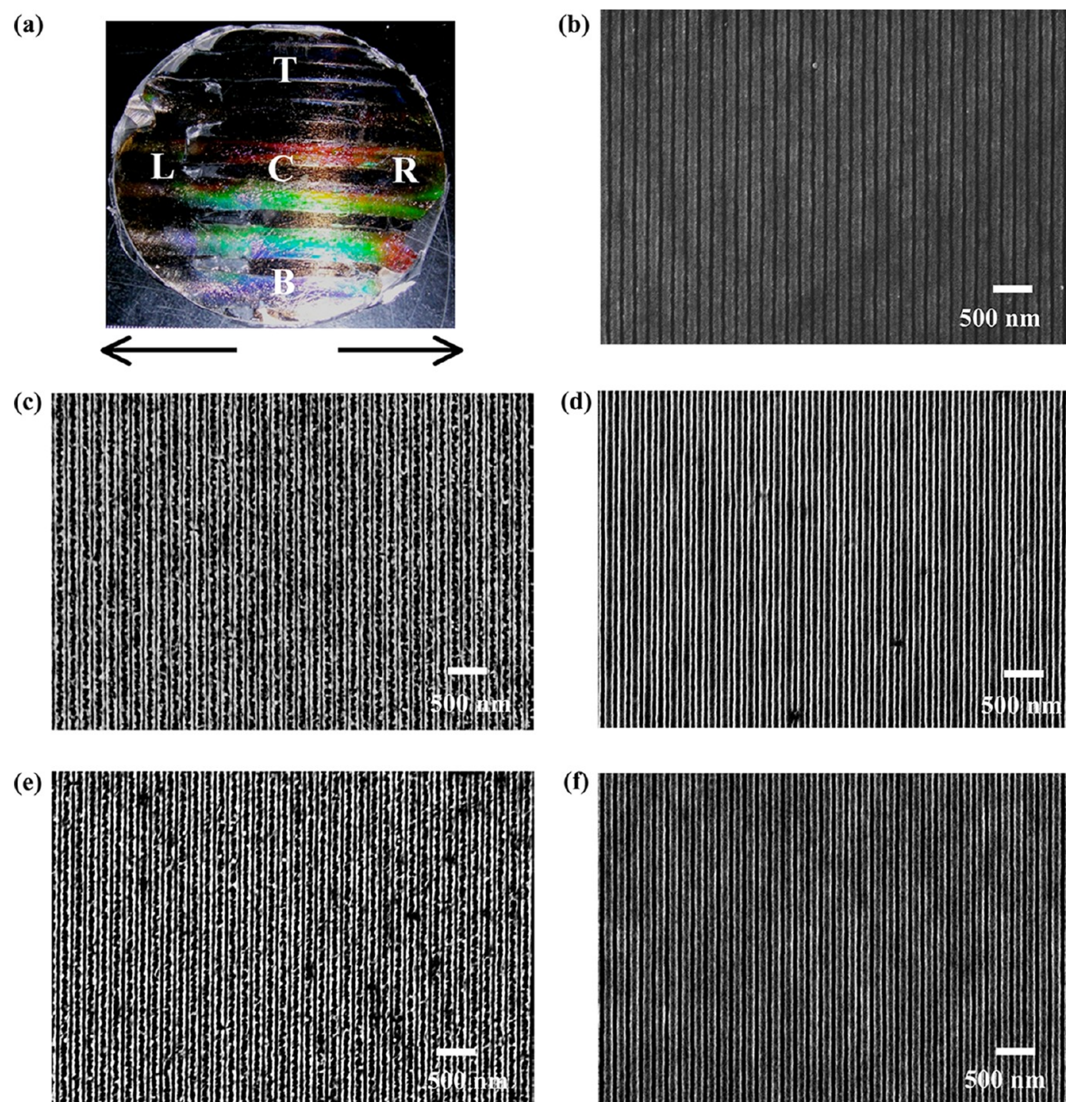

Figure 9. (a) Optical image of a large-area (10 cm long) PDMS substrate patterned with Al grating patterns. (b–f) SEM images of the Al grating patterns at the five different positions (C: center, T: top, B: bottom, L: left, R: right) of the PDMS substrate shown in (a).

salinization process of APTES, the adhesion between the Au and PDMS layers was significantly improved and the effective pattern transfer was achieved.

In recent years, Au nanostructures have drawn extensive interest due to the unconventional plasmonic properties. Well-ordered Au nanostructures with controlled feature size and shape can provide novel applications such as chemical sensing platforms[10] and metamaterials such as superlens.[11] In particular, there is an increasing interest in patterning Au nanostructures on flexible substrates for next generation low-weight and low-cost plasmonic devices.[8] The pattern transfer process of Au nanostructures on the PDMS substrate demonstrated in this study would advance such applications as nanophotonics and plasmonics.

Scotch-Tape Adhesion Test. The adhesion between the transferred metal film and the PDMS substrate has further been tested by using a scotch-tape. The scotch-tape peel test is a popular adhesion test performed for the characterization of the

dx.doi.org/10.1021/am301423s | *ACS Appl. Mater. Interfaces* 2012, 4, 5505–5514

thin film adhesion on a substrate.[43] Figure 7 shows the adhesion test performed on the Ti nanopore film (935 nm in pore periodicity) transferred onto a PDMS substrate. A new scotch tape with a size of 5 cm × 5 cm was applied on the metal surface with a size of 1 cm × 2 cm (Figure 7a). Mechanical pressure is applied by hands to enhance the adhesion of the tape to the metal surface (Figure 7b). Then the tape was quickly (<1 s) peeled off (Figure 7c). No Ti layer or residue was seen on the tape surface (Figure 7d), indicating a complete adhesion between the metal and PDMS layers.[43] Both tape and metal surfaces were further inspected under an optical microscope. No significant delamination and peeling of the Ti layer from the PDMS was observed. The metal surface was also examined with SEM. No noticeable damage or destruction of the Ti film and nanopore structures was observed (Figure 7e,f). The peel tests were repeated several times and the same results were obtained showing no apparent impairment of the structures. Nanograting patterns also showed similar peel test results. The scotch-tape peel tests were also performed with the nanopatterns of the other materials including Al, Ag, and Au, all showing complete adhesion.[43]

In mechanical applications of metallic nanostructures such as MEMS/NEMS and nanoimprint lithography, it is important to maintain good adhesion and structural robustness under forced conditions (e.g., by pressure or shear stresses). The results suggest that the metallic nanostructures fabricated by the proposed pattern transfer method would also be suitable for such applications.

Wet Immersion Test. The adhesion of the transferred metal film to the PDMS substrate has also been tested in wet environment. Figure 8 demonstrates such an immersion test in liquid water. The PDMS substrate (2 cm × 1 cm) patterned with the Ti nanopore structures (325 nm in periodicity) was immersed in deionized water for several days (Figure 8a). Even after being immersed for 7 days (Figure 8b), no significant delamination or detachment of the nanopatterned metal layer was observed (Figure 8c). Even when the sample was agitated in the water, no significant peeling was detected. The results further support good adhesion between the metal film and the PDMS layers. The wet immersion test was also performed in an organic solvent such as acetone. PDMS material can easily be swelled in organic solvents. However, no significant delamination of the transferred metal nanostructures on the PDMS surfaces was also observed even in testing with the organic solvent (see Figure S1 in Supporting Information). Similar results were obtained with the other metallic films (Al, Ag, and Au), including nanograting patterns.

Such a good adhesion and durability in a wet environment is critical in fluidics and biomedical applications such as micro-/nanofluidics, optofluidics, lab-on-a-chip, and implantable devices, where well-defined metallic nanostructures on the transparent and biocompatible PDMS substrate would enhance the functionality of the systems. In such applications, the metallic nanostructures should contact with liquid with hydraulic pressure and shear stresses. The results suggest that the metallic nanostructures created by the pattern transfer method would also be sustainable in both water and organic solvent based wet environment with associated fluid motions.

Scale-Up to Wafer-Level Pattern Transfer. The use of laser interference lithography has enabled the metallic nanostructures on a PDMS substrate to be fabricated up to a full wafer scale. By using a high-power Ar-ion laser of long coherence length (1.7 W and 1 m coherence length at 351.1 nm wavelength) and a large mirror size (4 in. × 4 in.) for the tunable Lloyd-mirror interferometer, the exposure area for nanopatterns was capable of covering a full 4-in. wafer (10 cm in diameter).[33] Figure 9 shows the Al nanograting patterns (200 nm in periodicity) created on a PDMS substrate (10 cm long) by using the PR nanopattern covering a full 4-in. Si wafer. The pattern uniformity and structural robustness were examined over the whole surface area. Figure 9b−f shows the SEM images taken at the five different locations (C: center, T: top, B: bottom, L: left, R: right) of the PDMS substrate shown in Figure 9a. The images confirm that the pattern periodicity of the nanograting metal structures is uniform over the entire surface area. No structural defect or crack/delamination of the film was observed over the surface, yielding pattern transfer fidelity of ∼100% over the surface area of 10 cm × 10 cm. Noticeable (<10%) variation of line width and edge roughness is detected in one corner of the boundary area (i.e., "L" and "B" regions, Figure 9c,e, respectively). It is because of the nonuniform contrast distribution over the PR mold layer at the exposure in the lithography step[33,44] and has little to do with the molding or peeling processes. The results indicate that the good adhesion between the metal and the PDMS layers is preserved even when the pattern transfer process is applied for the wafer-scale substrate size. Such scalability with robustness of the pattern transfer process will permit the low-cost high-throughput fabrication of metallic nanostructures over a large substrate area of PDMS material, offering new applicability even to full wafer-scale devices and systems.

Issues in Pattern Transfer of Pillar Nanostructures. Although successful pattern transfer of nanograting and nanopore metal structures was demonstrated in this study, it should be noted that in the case of transferring pillar-type metal nanostructures by using nanopore PR mold patterns, significant defects and destruction of the metal nanostructures were observed, yielding the pattern transfer fidelity of no more than 70% (see Figure S2 in Supporting Information). Especially when high-aspect-ratio nanopillar structures were fabricated, the metal pillar structures were stuck in the deep pores of the PR layer and typically broken at the base of the pillar structures in the mechanical peeling step. It is mainly attributed to the negatively tapered sidewall profile of the nanopore PR structures made of negative-tone PR material. The adverse sidewall profile makes the base region of the deposited metal pillar structures slenderer and mechanically weak so that mechanical fracturing typically occurs at the peeling process. Moreover, if the aspect ratio of the PR pore structures (the ratio of the pore depth to the pore diameter) was greater than ∼3, it was difficult to deposit the metal film to completely fill the pores due to the step coverage issue and the formation of keyhole-shaped voids. Thus, the precise pattern transfer of the pillar-type nanostructures with high fidelity currently remains an issue.

Instead of the direct mechanical peeling, it was examined to use PR etchants to remove the PR layer before the separation of the metal/PDMS layers from the Si substrate. However, the etchant solution of the PR material seriously attacks the PDMS substrate and results in the delamination of the metal film from the PDMS substrate.

4. CONCLUDING REMARKS

In past decades, the pattern transfer approach based on soft lithographic techniques using PDMS elastomer material has drawn great interest in micro- and nanofabrication because of

the low-cost and simple fabrication process required. By using the soft lithographic pattern transfer method, fabrication process can conveniently be carried out in ambient environment. In this paper, we have demonstrated that a direct molding and peeling of the elastomeric PDMS substrate over the thin metal films predeposited on a nanostructured photoresist layer allows the simple and effective replication and pattern transfer of the metallic nanostructures onto the PDMS surface. In the pattern transfer approach based on the molding process, the adhesion or surface energy competition between the template and target substrates (photoresist and PDMS in this study) to the metal material is the key process parameter. In typical pattern transfer processes, target substrates are normally made to have better adhesion or higher surface energy compared to the template substrate. For such treatment, heat and pressure are often applied in order to increase the adhesion between the metallic layer and target substrates. Also, adhesion (to the target substrate) or antiadhesion (to the template substrate) coatings/layers are generally applied in the fabrication processes to improve the output of the pattern transfer. The new pattern transfer process investigated in this paper reveals that most metallic films (Ti, Al, and Ag) do not require such treatment for the regulation of adhesion to either side of the photoresist (template layer) or PDMS (target substrate).

The advanced pattern transfer process developed in this study has several advantages over the other techniques reported so far. First of all, it allows the wafer-scale large-area pattern transfer by using the holographic lithography in the preparation of the photoresist mold layer. It is a fast and inexpensive process compared to other nanolithography techniques. It also enables the sidewall profile of the PR nanostructures to be tailored (e.g., to be positively tapered in case of using positive-tone photoresist material) so that the pattern transfer can be achieved by a simple mechanical peeling process. The use of the soft photoresist material as a direct mold structure also simplifies the fabrication process and enhances the transferability, compared to the conventional pattern transfer approaches using hard and rigid substrate materials as the template layer. Furthermore, such photoresist templates can also be reused after the pattern transfer, allowing repetitive replication and pattern transfer processes. The feature size and shape of transferred metallic nanostructures can be defined by photoresist template, without losing the precision from making additional molds. In this study, the pattern transfer of metal nanostructures of grating and pore patterns with minimum lateral feature size down to ∼100 nm and the maximum aspect ratio up to ∼5 was demonstrated successfully (fidelity of ∼100% over 10 cm × 10 cm substrate area). Second, the metallic nanostructures are directly formed on the photoresist patterns via a thin film deposition process, which avoids much complexity associated with the other fabrication methods such as plasma-based dry etching of metallic materials. The pattern transfer method using deposition techniques over the prepatterned soft template layer is ideal to fabricate metal nanostructures of a wide range of metallic materials. Such metallic nanostructures robustly built on flexible and transparent substrates such as PDMS with a large pattern coverage area up to a full wafer scale will advance many scientific and engineering applications such as micro-/nanofluidics, optofluidics, plasmonics, nanophotonics, and nanoelectronics.

ASSOCIATED CONTENT

Supporting Information

The result of the immersion adhesion test performed in an organic solvent (acetone) is shown in Figure S1. The scanning electron microscope (SEM) images of aluminum (Al) nanopillar structures (325 nm in periodicity) transferred onto a PDMS substrate are shown in Figure S2. This material is available free of charge via the Internet at http://pubs.acs.org.

AUTHOR INFORMATION

Corresponding Author

*Phone: 201-216-5579. Fax: 201-216-8315. E-mail: cchoi@stevens.edu.

Notes

The authors declare no competing financial interest.

ACKNOWLEDGMENTS

This research was carried out in part at the Center for Functional Nanomaterials (CFN), Brookhaven National Laboratory (BNL), which was supported by the U.S. Department of Energy, Office of Basic Energy Sciences, under Contract No. DE-AC02-98CH10886. The authors thank Dr. Ming Lu at the BNL for help with using the nanofabrication facility at the CFN. The research effort used microscope resources partially funded by the National Science Foundation through NSF Grant DMR-0922522. The authors also thank Dr. Tsengming Chou at the Stevens Institute of Technology for the assistance with FIB milling.

REFERENCES

(1) O'Brien, M. J.; Bisong, P.; Ista, L. K.; Rabinovich, E. M.; Garcia, A. L.; Sibbett, S. S.; Lopez, G. P.; Brueck, S. R. J. *J. Vac. Sci. Technol. B* **2003**, *21*, 2941−2945.

(2) Garcia, A. L.; Ista, L. K.; Petsev, D. N.; O'Brien, M. J.; Bisong, P.; Mammoli, A. A.; Brueck, S. R. J.; Lopez, G. P. *Lab Chip* **2005**, *5*, 1271−1276.

(3) Craighead, H. G. *Science* **2000**, *290*, 1532−1535.

(4) Chen, C. M.; Sung, C. K. *Microelectron. Eng.* **2010**, *87*, 872−875.

(5) Tan, H.; Gilbertson, A.; Chou, S. Y. *J. Vac. Sci. Technol. B* **1998**, *16*, 3926−3928.

(6) Yang, J. C.; Gao, H. W.; Suh, J. Y.; Zhou, W.; Lee, M. H.; Odom, T. W. *Nano Lett.* **2010**, *10*, 3173−3178.

(7) Lindquist, N. C.; Johnson, T. W.; Norris, D. J.; Oh, S. H. *Nano Lett.* **2011**, *11*, 3526−3530.

(8) Tao, H.; Amsden, J. J.; Strikwerada, A. C.; Fan, K.; Kaplan, D. L.; Zhang, X.; Averitt, R. D.; Omenetto, F. G. *Adv. Mater.* **2010**, *22*, 3527−3531.

(9) Deng, X. G.; Braun, G. B.; Liu, S.; Sciortino, P. F.; Koefer, B.; Tombler, T.; Moskovits, M. *Nano Lett.* **2010**, *10*, 1780−1786.

(10) Choi, C. J.; Xu, Z.; Wu, H. Y.; Liu, G. L.; Cunningham, B. T. *Nanotechnology* **2010**, *21*, 415301.

(11) Lee, M. H.; Huntington, M. D.; Zhou, W.; Yang, J.-C.; Odom, T. W. *Nano Lett.* **2010**, *10*, 311−315.

(12) Kim, D. H.; Liu, Z. J.; Kim, Y. S.; Wu, J.; Song, J. Z.; Kim, H. S.; Huang, Y. G.; Hwang, K. C.; Zhang, Y .W.; Rogers, J. A. *Small* **2009**, *5*, 2841−2847.

(13) Ko, H. C.; Shin, G. C.; Wang, S. D.; Stoykovich, M. P.; Lee, J. W.; Kim, D. H.; Ha, J. S.; Huang, Y. G.; Hwang, K. C.; Rogers, J. A. *Small* **2009**, *5*, 2703−2709.

(14) Kim, S.; Su, Y.; Mihi, A.; Lee, S.; Liu, Z.; Bhandakkar, T. K.; Wu, J.; Geddes, J. B.; Johnson, H. T.; Zhang, Y.; Park, J.; Braun, P.; Huang, Y.; Rogers, J. A. *Small* **2012**, *8*, 901−906.

(15) Song, J.; Jiang, H.; Huang, Y.; Rogers, J. A. *J. Vac. Sci. Technol. A* **2009**, *27*, 1107−1125.

(16) Fujii, T. *Microelectron. Eng.* **2002**, *61−62*, 907−914.

(17) Engelmark, F.; Iriarte, G. F.; Katardjiev, I. V. *J. Vac. Sci. Technol. B* **2002**, *20*, 843−848.
(18) Aimi, M. F.; Rao, M. P.; Macdonald, N. C.; Zuruzi, A. S.; Bothman, D. P. *Nat. Mater.* **2004**, *3*, 103−105.
(19) Guo, L.; DeWeerth, S. P. *Small* **2010**, *6*, 2847−2852.
(20) Sabella, S.; Shiv Shankar, S.; Vecchio, G.; Brunetti, V.; Rizzello, L.; Qualtieri, A.; Martiradonna, L.; Cingolani, R.; Pompa, P. P. *Mater. Lett.* **2010**, *64*, 41−44.
(21) Fakhr, O.; Altpeter, P.; Karrai, K.; Lugil, P. *Small* **2011**, *7*, 2533−2538.
(22) Aldakov, D.; Tondelier, D.; Palacin, S.; Bonnassieux, Y. *ACS Appl. Mater. Interfaces* **2011**, *3*, 740−745.
(23) Gou, H.; Xu, J.; Xia, X.; Chen, H. *ACS Appl. Mater. Interfaces* **2010**, *2*, 1324−1330.
(24) Basarir, F. *ACS Appl. Mater. Interfaces* **2012**, *4*, 1324−1329.
(25) Du, K.; Wathuthanthri, I.; Xu, W.; Mao, W.; Choi, C.-H. *Nanotechnology* **2011**, *22*, 285306.
(26) Chen, C.-H.; Yu, T.-H.; Lee, Y.-C. *J. Micromech. Microeng.* **2010**, *20*, 025034.
(27) Chen, C.-H.; Yu, T.-H.; Lee, Y.-C. *J. Microelectromech. Syst.* **2011**, *20*, 916−921.
(28) Kwak, M. K.; Kim, T.; Kim, P.; Lee, H. H.; Suh, K. Y. *Small* **2009**, *5*, 928−932.
(29) Kwak, M. K.; Shin, K. H.; Yoon, E. Y.; Suh, K. Y. *J. Colloid Interface Sci.* **2010**, *343*, 301−305.
(30) Smith, H. *Physica E* **2001**, *11*, 104−109.
(31) Fernandez, A.; Nguyen, H. T.; Britten, J. A.; Boyd, R. D.; Perry, M. D.; Kania, D. R.; Hawryluk, A. M. *J. Vac. Sci. Technol. B* **1997**, *15*, 729−735.
(32) Zuppella, P.; Luciani, D.; Tucceri, P.; De Marco, P.; Gaudieri, A.; Kaiser, J.; Ottavano, L.; Santucci, S.; Reale, A. *Nanotechnology* **2009**, *20*, 115303.
(33) Wathuthanthri, I.; Mao, W.; Choi, C.-H. *Opt. Lett.* **2011**, *36*, 1593−1595.
(34) Wathuthanthri, I.; Liu, Y.; Du, K.; Xu., W.; Choi, C.-H. *Adv. Funct. Mater.* **2012**, DOI: 10.1002/adfm.201201814.
(35) Ouellet, E.; Yang, C. W. T.; Lin, T.; Yang, L. L.; Lagally, E. T. *Langmuir* **2010**, *26*, 11609−11614.
(36) Lacoura, S. P.; Wagner, S.; Huang, Z.; Suo, Z. *Appl. Phys. Lett.* **2003**, *82*, 2404−2406.
(37) Loo, Y. L.; Willett, R. L.; Baldwin, K. W.; Rogers, J. A. *J. Am. Chem. Soc.* **2002**, *124*, 7654−7655.
(38) Loo, Y. L.; Willett, R. L.; Baldwin, K. W.; Rogers, J. A. *Appl. Phys. Lett.* **2002**, *81*, 562−564.
(39) Lim, K. S.; Chang, W. J.; Koo, Y. M.; Bashir, R. *Lab Chip* **2006**, *6*, 578−580.
(40) Schuy, S.; Janshoff, A. *J. Colloid Interface Sci.* **2006**, *295*, 93−99.
(41) Ballarin, B.; Cassani, M. C.; Gazzano, M.; Solinas, G. *Electrochim. Acta* **2010**, *56*, 676−686.
(42) Freeman, R. G.; Grabar, K. C.; Allison, K. J.; Bright, R. M.; Davis, J. A.; Guthrie, A. P.; Hommer, M. B.; Hackson, M. A.; Smith, P. C.; Walter, D. G.; Natan, M. J. *Science* **1995**, *267*, 1629−1632.
(43) Hidber, P. C.; Helbig, W.; Kim, E.; Whitesides, G. M. *Langmuir* **1996**, *12*, 1375−1380.
(44) Mao, W.; Wathuthanthri, I.; Choi, C.-H. *Opt. Lett.* **2011**, *36*, 3176−3178.